

How well do we know the age and mass distributions of the star cluster system in the Large Magellanic Cloud?

Richard de Grijs¹* and Peter Anders²

¹ Department of Physics & Astronomy, The University of Sheffield, Hicks Building, Hounsfield Road, Sheffield S3 7RH

² Institut für Astrophysik, Georg-August-Universität, Friedrich-Hund-Platz 1, 37077 Göttingen, Germany

Received date; accepted date

ABSTRACT

The Large Magellanic Cloud (LMC) star cluster system offers the unique opportunity to independently check the accuracy of age (and the corresponding mass) determinations based on a number of complementary techniques. Using our sophisticated tool for star cluster analysis based on broad-band spectral energy distributions (SEDs), “AnalySED”, we reanalyse the Hunter et al. (2003) LMC cluster photometry. Our main aim is to set the tightest limits yet on the accuracy of *absolute* age determinations based on broad-band SEDs, and therefore on the usefulness of such an approach. Our broad-band SED fits yield reliable ages, with statistical absolute uncertainties within $\Delta \log(\text{Age}/\text{yr}) \simeq 0.4$ overall. The systematic differences we find with respect to previous age determinations are caused by conversions of the observational photometry to a different filter system, thus leading to systematically inaccurate results.

The LMC’s cluster formation rate (CFR) has been roughly constant outside of the well-known age gap between ~ 3 and 13 Gyr, when the CFR was a factor of ~ 5 lower. Using a simple approach to derive the characteristic cluster disruption time-scale, we find that $\log(t_4^{\text{dis}}/\text{yr}) = 9.9 \pm 0.1$, where $t_{\text{dis}} = t_4^{\text{dis}}(M_{\text{cl}}/10^4 M_{\odot})^{0.62}$. This long characteristic disruption time-scale implies that we are observing the *initial* cluster mass function (CMF). We conclude that while the older cluster (sub)samples show CMF slopes that are fully consistent with the $\alpha \simeq -2$ slopes generally observed in young star cluster systems, the youngest mass and luminosity-limited LMC cluster subsets show shallower slopes (at least below masses of a few $\times 10^3 M_{\odot}$), which is contrary to dynamical expectations. This may imply that the initial CMF slope of the LMC cluster system as a whole is *not* well represented by a power-law, although we cannot disentangle the unbound from the bound clusters at the youngest ages.

Key words: methods: data analysis, Magellanic Clouds, galaxies: star clusters, galaxies: stellar content

1 INTRODUCTION

The debate regarding the true underlying mass function of young star cluster systems is presently very much alive, because it bears on the very essence of the star-forming process, as well as on the formation, assembly history and evolution of the clusters’ host galaxies over cosmic time. Although observational evidence of young cluster systems in many star cluster-forming interacting and starburst galaxies appears to indicate that they are well represented by power-law cluster *luminosity* functions (CLFs; see de Grijs et al. 2003d for a recent comprehensive review), rapid changes to the stellar population properties, combined with a (possibly significant) age range within a given cluster system may

conspire to give rise to a power-law-like CLF, even if the true underlying cluster *mass* function (CMF) is not a power law (Meurer 1995; Miller et al. 1997; Fritze-v. Alvensleben 1998, 1999; de Grijs et al. 2001, 2003a,b; Hunter et al. 2003, hereafter H03). It is, therefore, obviously very important to age date the individual clusters and to correct the observed CLF to a common age, before interpreting the cluster luminosities in terms of the corresponding mass distribution (Fritze-v. Alvensleben 1999; de Grijs et al. 2001, 2003a,b; H03). This is particularly important if the age spread within a cluster system is a significant fraction of the system’s mean age.

Even with the high spatial resolution offered by the advanced suite of instruments onboard the *Hubble Space Telescope*, extragalactic star clusters at distances beyond the Local Group can only be studied through their integrated

* E-mail: R.deGrijs@sheffield.ac.uk

properties. However, we *do* have access to a statistically significant young to intermediate-age *resolved* star cluster system on our doorstep, notably in the Large Magellanic Cloud (LMC). By combining *integrated* properties with *resolved* stellar population studies, the LMC cluster system offers the unique chance to independently check the accuracy of age (and corresponding mass) determinations based on broad-band spectral energy distributions (SEDs). This is what we set out to do in this paper, based on the largest, most homogeneous and complete set of integrated LMC cluster photometry presently available. With our new cluster age estimates, spanning ages from a few Myr up to 10 Gyr, determined in an internally consistent fashion and with a firm handle on the associated uncertainties, we now also have the largest, homogeneous sample of cluster masses with well-defined uncertainties to date, which we use to explore the evolution of the CMF.

In Section 2 we discuss the details of the LMC cluster sample we base our analysis on, and explore the uncertainties associated with the age and mass determinations. Section 3 discusses the formation and disruption history of the LMC star cluster sample. We use this as our basis for the interpretation of the LMC cluster mass distribution in terms of the initial and evolved distributions of cluster masses in Section 4. Finally, in Section 5 we summarise our results and conclusions.

2 DATA AND ACCURACY ANALYSIS

The basis for our detailed comparison of the age estimates for the LMC star cluster system is provided by (i) the *UBVR* broad-band SEDs of H03, based on Massey's (2002) CCD survey of the Magellanic Clouds, and (ii) the OGLE-II data set (Udalski, Kubiak & Szymański 1997), and in particular their homogeneously determined ages for some 600 clusters, using colour-magnitude diagrams (CMDs; Pietrzyński & Udalski 2000).

H03 determined the ages for the individual LMC clusters by comparing their broad-band SEDs with a variety of cluster evolutionary models. Specifically, they used the Starburst99 (Leitherer et al. 1999) with $Z = 0.008$ for ages up to 1 Gyr, while for older ages they used a combination of the *UBV* colours of Searle, Sargent & Bagnuolo (1973), the $(V - R)_C$ colours for globular clusters from Reed (1985), and the Charlot & Bruzual (1991) simple stellar population (SSP) models for the evolution of the *V*-band luminosity in the age range from 1 to 10 Gyr. They then used a combination of two colour-colour diagrams, $(U - B)$ vs. $(B - V)$ and $(B - V)$ vs. $(V - R)$, to obtain their age estimates, by comparing the cluster positions to the model tracks in those diagrams.

The colours and magnitudes of their sample clusters were corrected for reddening using a blanket reddening of $E(B - V) = 0.13$ mag for all clusters, where they adopted the extinction curve of Cardelli et al. [1989; $R_V \equiv Av/E(B - V) = 3.10$].

The Pietrzyński & Udalski (2000) ages are based on detailed isochrone fits to the OGLE-II colour-magnitude data, using the Padova isochrones for $Z = 0.008$. They dereddened their photometry using the extinction values for 84 LMC subfields determined by Udalski et al. (1999),

$E(B - V) = 0.143 \pm 0.020$ mag. These extinction values are based on Schlegel et al.'s (1998) reddening maps for the Galactic foreground extinction, on average $E(B - V) = 0.075$ mag, and their $R_V = 3.24$.

Finally, here we reanalyse the Massey (2002) data set, also assuming $Z = 0.008$, for comparison purposes (although our analysis tool allows us to leave the metallicity as a free parameter; see Section 2.2). For the total extinction towards the LMC clusters, we assumed $E(B - V) = 0.10$ mag, using the Calzetti attenuation law (Calzetti 1997, 2001; Calzetti et al. 2000; Leitherer et al. 2002) with $R_V = 4.05$. This corresponds to $E(B - V) \simeq 0.13$ mag for both the Cardelli et al. (1989) and the Schlegel et al. (1998) extinction laws.

In a series of recent papers, we developed a sophisticated tool for star cluster analysis based on broad-band SEDs, "AnalySED", which we tested extensively both internally (de Grijs et al. 2003c,d; Anders et al. 2004) and externally (de Grijs et al. 2005), using both theoretical and observed young to intermediate-age ($t \lesssim 3 \times 10^9$ yr) star cluster SEDs, and the GALEV SSP models (Kurth et al. 1999; Schulz et al. 2002). We increased the accuracy for younger ages by the inclusion of an extensive set of nebular emission lines, as well as gaseous continuum emission (Anders & Fritze-v. Alvensleben 2003). We concluded that the *relative* ages within a given cluster system can be determined to a very high accuracy depending on the specific combination of passbands used (Anders et al. 2004). Even when comparing the results of different groups using the same data set, we can retrieve prominent features in the cluster age distribution to within $\sigma_t \equiv \Delta \langle \log(\text{Age}/\text{yr}) \rangle \leq 0.35$ (de Grijs et al. 2005), which confirms that we understand the uncertainties associated with the use of our AnalySED tool to a very high degree.

The aim of this section is to compare our new age determinations with (i) those of H03 using the same data set but a different approach, and (ii) those of Pietrzyński & Udalski (2000) using the independent (and presumably more accurate) method of CMD fitting. This will allow us to set the tightest limits yet on the accuracy of *absolute* age determinations based on broad-band SEDs, and therefore on the usefulness of such an approach in general.

First, we compare the independently determined ages of the clusters in common between the H03 and OGLE-II results. Fig. 1a shows the distribution of the data points in the relevant parameter space, where the dashed line represents equality between both age estimates for a given cluster. It is immediately clear that there is a systematic difference between the H03 and OGLE-II ages, the magnitude of which is a clear function of age. The effect is indeed significant; a straightforward linear regression results in a slope that is significantly different from unity, 1.47 ± 0.07 . We will explore the origin of this systematic effect in Section 2.1 below. It is also clear that, in units of $\log(\text{Age}/\text{yr})$, the intrinsic scatter in the data points is somewhat greater at younger ages; this is merely an effect of the poorer intrinsic age accuracy for older ages imposed by the models.

Secondly, we compare our redetermined ages to both those of OGLE-II and H03, in Figs. 1b and c, respectively. We point out that because of the limiting *V*-band magnitude of the OGLE-II data, their age estimates are only reliable for ages $\lesssim 1$ Gyr. Consequently, the comparison between the OGLE-II CMD-based ages and our age determinations in this paper are only valid for ages $\lesssim 1$ Gyr, as is also evident

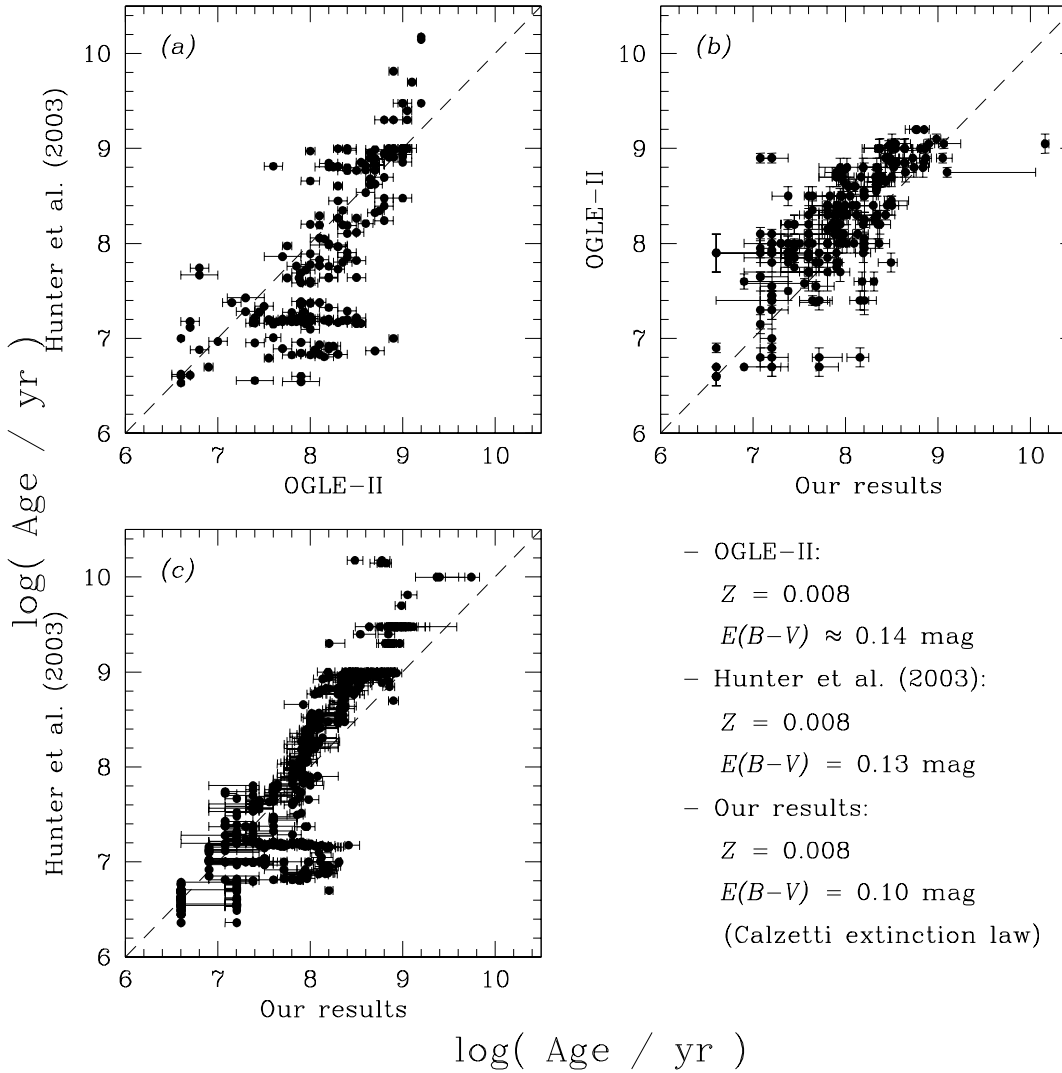


Figure 1. Comparison of age determination for LMC clusters in common between Hunter et al. (2003), the OGLE-II team of Pietrzyński & Udalski (2000), and this paper. The assumptions on the overall metallicity and extinction properties of the cluster sample are indicated in the legend.

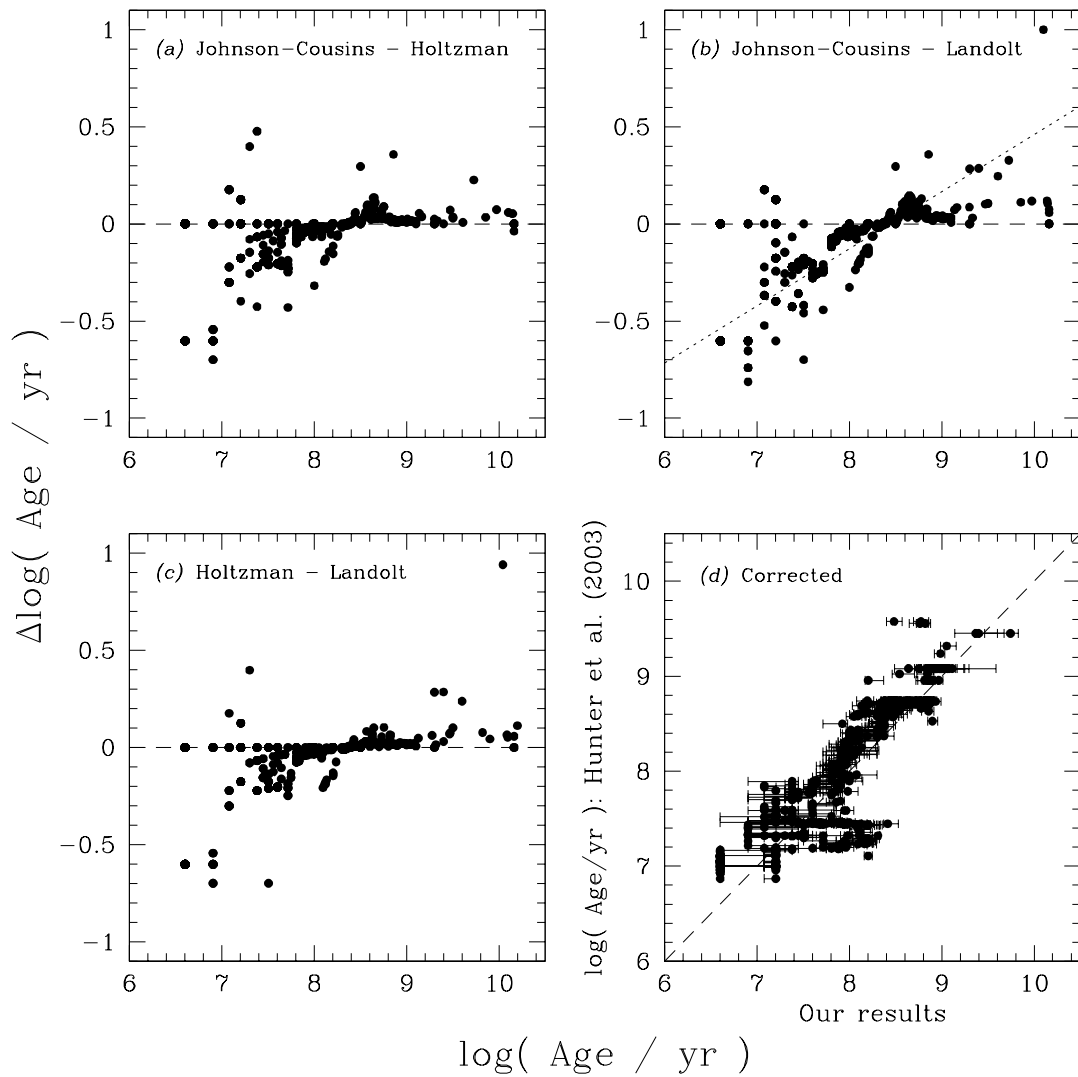
from the lack of data points for $\log(\text{Age}/\text{yr}) \gtrsim 9.0$ in Fig. 1b. For the older sample clusters, for which age estimates are available based on spectral features or CMD analysis, the comparison is extended on a one-by-one basis in Section 2.3.

The systematic effect shown by the H03 data seems to have disappeared when we compare our results to those of the OGLE-II team; the resulting slope is 1.05 ± 0.05 , with an x-axis intercept at $\log(\text{Age}/\text{yr}) = -0.11 \pm 0.39$. This excellent agreement indicates that our assumption that the overall extinction is well represented by $E(B-V) = 0.10$ mag (assuming the Calzetti attenuation law) is well justified; a change in extinction of $|\Delta E(B-V)| = 0.05$ would correspond to an offset from the line of equality of $|\Delta \log(\text{Age}/\text{yr})| \simeq 0.10$. This effect is a direct result of the age-extinction, and possibly (to a lesser extent) also of the age-metallicity degeneracy (see Section 2.2). The systematic effect with respect to the H03 results is still visible, although the scatter in the results

is – perhaps not surprisingly because we used the same data set – much smaller than when we compare our results to those of OGLE-II. Table 1 contains the full numerical details for a quantitative comparison among the age determinations based on the samples discussed here. We note that any remaining offset between our results and those of the OGLE-II team, despite having used the same assumptions for the total extinction towards the clusters, may have been introduced by the exact value for the distance modulus assumed by Pietrzyński & Udalski (2000), $m - M = 18.23$ mag, which is an essential ingredient for age determinations based on CMD fitting. If they had assumed a nominal $m - M = 18.50$ mag, their resulting age estimates would have been younger by $\Delta \log(\text{Age}/\text{yr}) \sim 0.2 - 0.4$, depending on the age range considered (larger offsets result for younger ages).

Table 1. Quantitative comparison among age determinations.

Source 1	Source 2	Slope	Intercept [log(Age/yr)]	Scatter, $\langle \sigma_t \rangle$ [($\Delta \log(\text{Age/yr})$)]	Correlation coefficient, \mathcal{R}
OGLE-II	H03	1.44 ± 0.07	-3.85 ± 0.61	0.62	0.74
OGLE-II	H03 (corrected)	1.04 ± 0.05	-0.47 ± 0.44	0.44	0.74
This paper	OGLE-II	1.05 ± 0.05	-0.11 ± 0.39	0.42	0.74
This paper	H03	1.38 ± 0.03	-2.96 ± 0.20	0.47	0.88
This paper	H03 (corrected)	0.98 ± 0.02	0.23 ± 0.14	0.33	0.88

**Figure 2.** (a)–(c) The effects of colour transformations between filter systems on the derived ages for the Massey (2002) LMC cluster photometry, assuming $Z = 0.008$ and $E(B - V) = 0.10$ mag. We have chosen to omit the formal uncertainties on the data points for reasons of clarity. (d) Comparison of the corrected age determinations for the H03 sample to our redeterminations in this paper.

2.1 Filter transmission curves

In the previous section we noted a significant systematic effect between the age differences of H03 on the one hand, and those of both the OGLE-II team and our own redeterminations on the other. H03 converted the Starburst99 Johnson ($V - R$) colour to the Cousins system. As we showed in de Grijs et al. (2005; their figs. 10 and 11), filter conversions

may be responsible for significant differences in the resulting age determinations. In order to investigate the possibility of this effect playing a role for these data, we carefully analysed the properties of the original and converted systems used. Massey (2002) calibrated his photometry using the Landolt (1992) standard stars, so that his photometry should be analysed using the filter set used to obtain the standard-star photometry. The Landolt (1992) filter curves

are very close to the filter transmission curves used by Holtzman et al. (1995), who also kindly supplied us with the original, unpublished Landolt KPNO curves (J. Holtzman, priv. comm.). For completeness, we will therefore assess the differences in the resulting ages for our LMC cluster sample based on using the “standard” Johnson-Cousins system (as done by H03), the curves used by Holtzman et al. (1995), and the original KPNO curves used by Landolt (1992).

The results of this are shown in Fig. 2. Fig. 2c shows that the filter transmission curves used by Holtzman et al. (1995) and Landolt (1992), respectively, indeed yield relatively similar age estimates. The most important comparison figure is displayed in panel b, however. The systematic trend seen here mimics that seen in Figs. 1a and c, in the sense that if one uses the Johnson-Cousins filter system (even if based on the appropriate conversion equations) instead of the native Landolt KPNO system, one will obtain lower ages than expected at the young-age end of the age range covered by our LMC cluster sample, and vice versa. To provide further evidence for this scenario, we applied a simple linear regression to the data points in Fig. 2c (shown by the dotted line), and applied the resulting equation as a first-order correction to H03’s age determinations in both Figs. 1a and c. The resulting, corrected age comparison is shown in Fig. 2d, while the numerical values are once again included in Table 1. It thus appears that the systematic differences in LMC cluster ages between the H03 results and those of OGLE-II and ourselves are indeed caused by their conversions of the photometry to a different filter system.

2.2 The age-metallicity and age-extinction degeneracies

In the discussion of our results, we have thus far assumed a fixed metallicity of $Z = 0.008$ and a fixed extinction of $E(B - V) = 0.10$ mag (assuming the Calzetti attenuation law) for all of our sample clusters. The AnalySED tool has been developed to also provide independent information on a cluster’s metallicity and extinction, provided that a significant number of data points defining the SED are available to match the number of free parameters (cf. de Grijs et al. 2003c,d; Anders et al. 2004).

Therefore, we have also reanalysed the LMC cluster photometry assuming (i) variable metallicity and $E(B - V) = 0.10$ mag, (ii) $Z = 0.008$ and variable extinction, and (iii) variable extinction and metallicity, the results of which are shown in Figs. 3a, b and c, respectively. From close scrutiny of these panels, it appears that the age-metallicity degeneracy is least important *for this cluster sample*; this implies that the assumption of $Z = 0.008$ adopted by H03, OGLE-II and ourselves in the previous sections is a reasonable approximation of the average LMC cluster metallicity. We also note that adopting $Z = 0.008$ as a reasonable approximation for the average cluster metallicity is supported – at least for clusters younger than ~ 3 Gyr – by a number of spectroscopic studies based on individual cluster stars (see, e.g., Olszewski et al. 1991, their fig. 11).

The effects of the age-extinction degeneracy are dramatic for this sample, however. On average, we find that if we had not assumed a fixed extinction value, the resulting ages would have been smaller (although there remains significant scatter about the dashed line of equality). However,

we caution that some of this scatter is likely artificial; as we showed in de Grijs et al. (2003d), the age-extinction degeneracy is artificially worsened (in the sense that clusters are artificially assigned younger ages) if the wavelength baseline used for the multi-parameter cluster SED analysis lacks wavelength coverage longward of the R filter, as is the case here. In essence, this is shown by the enhanced population of the two youngest age bins (at 4 and 8 Myr) in Figs. 3b and c for the models without restrictions on $E(B - V)$. This situation can be avoided successfully by adopting a fixed value for either the cluster population’s (average) extinction or metallicity (de Grijs et al. 2003d).

Thus, in view of these considerations, this implies that our results are indeed very comparable to those obtained from the OGLE-II data.

2.3 Other comparisons

Finally, to assess the robustness of the individual ages, we compare the LMC cluster age determinations of H03 (uncorrected), OGLE-II and ourselves with those obtained for smaller cluster samples using a variety of techniques. In Fig. 4 we have included those samples containing ≥ 5 clusters in common with our sample for which the authors determined their ages based on broad-band photometry. With the exception of the Meurer et al. (1990) results, who used the ultraviolet colours $C(18 - 31)_0$ and $C(25 - 31)_0$, all other age determinations are based on blue optical colours. Bica et al. (1986, 1990) used the $C(43 - 45)_0$ vs. $C(45 - H\beta)_0$ vs. SWB type (Searle, Wilkinson & Bagnuolo 1980) diagnostics, while Chiosi et al. (1988; UBV colours) and Santos et al. (1995; $(U - B)_0$ colours) limited themselves to the “standard” set of broad-band filters.

Although the Meurer et al. (1990) ages are clearly systematically greater than any of the ages determined by H03, OGLE-II or us, the other age determinations are statistically similar to those discussed elsewhere in this paper. This is encouraging regarding the robustness of our results; the relatively large scatter is a side effect of the poor age resolution for broad-band colours only. The fact that Meurer et al.’s (1990) ultraviolet-based age determinations are clearly greater than ours underscores the difficulties involved in using this wavelength range alone for age determinations. The main uncertainties inherent to this at ultraviolet wavelengths are the uncertain stellar population synthesis and uncertain extinction corrections.

In Fig. 5 we show a similar comparison between the ages discussed elsewhere in this paper, and those obtained independently based on spectral features or CMD fits. The similarities between our and H03’s broad-band SED fits and the OGLE-II fits on the one hand, and the determinations from the literature are striking, as is the relatively small scatter about the (dashed) lines of equality. Both the simplest of these age determinations, Elson & Fall’s (1988) ages based on the clusters’ main-sequence turn-off magnitudes (assuming a common distance to their entire sample), as well as the CMD fits by Olszewski et al. (1991) and Vallenari et al. (1998), and the more sophisticated determinations based on distinct spectral features by Beasley et al. (2002; see figure legend) and Santos & Piatti (2004; based on equivalent width measurements of the integrated spectra) match our broad-band SED ages very well. We also emphasize that

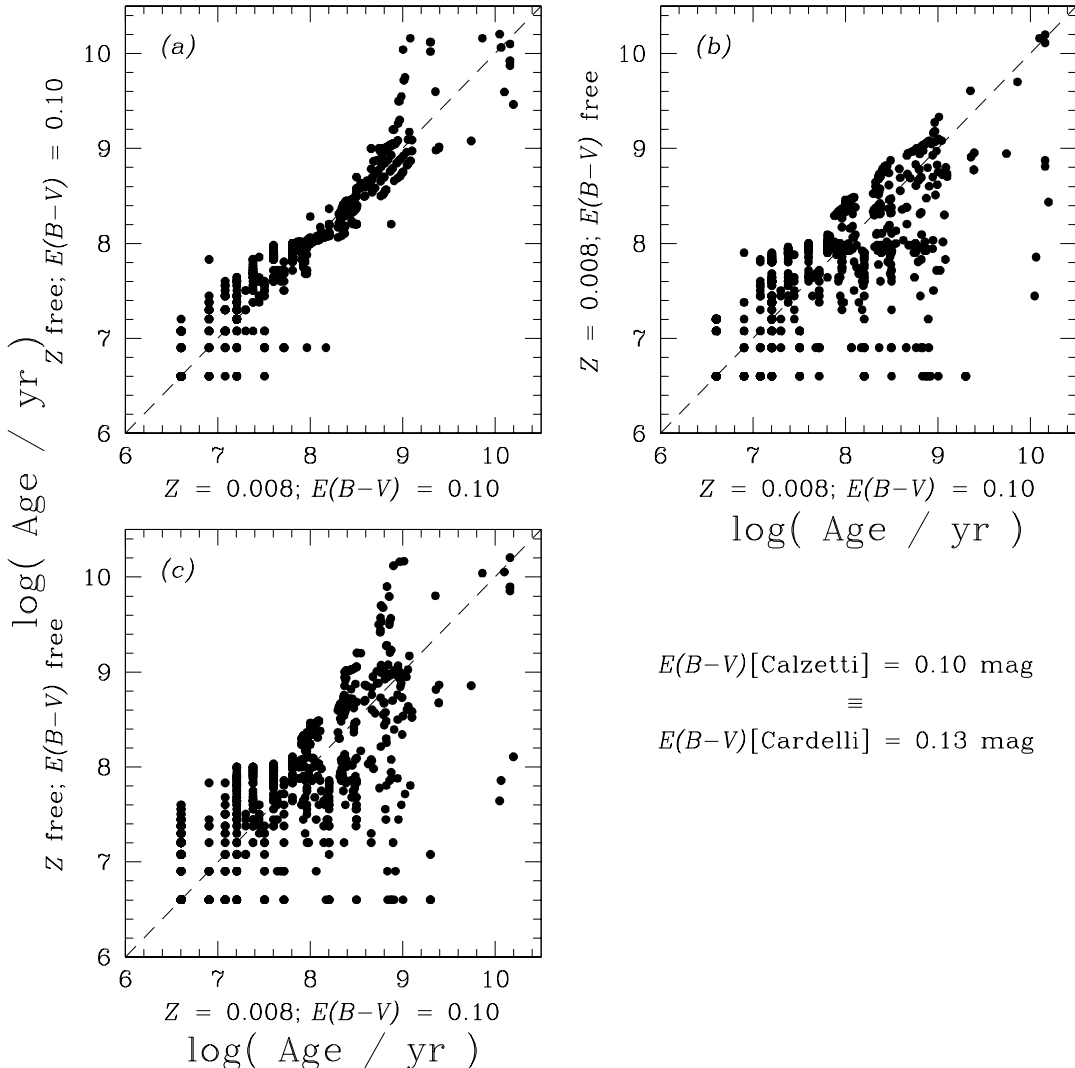


Figure 3. The effects of (a) the age-metallicity, (b) the age-extinction, and (c) the combined degeneracies. Again, error bars have been omitted for reasons of clarity.

Barbaro & Olivi's (1991) ages based on ultraviolet *spectra* return reliable ages, as opposed to those based on the ultraviolet *colours* discussed in relation to Fig. 4. H03, based on a comparison involving fewer objects taken from the literature, also concluded that the general match between their results and CMD-based ages was satisfactory, although they stated that for the oldest cluster colours tend to underestimate the ages compared to CMD fits. However, we have now shown that most (but possibly not all; see below) of this discrepancy was most likely caused by the systematic effects introduced by the filter conversion they employed. The small number of clusters available for this comparison (and the smaller number used by H03) did not allow H03 to notice the systematic offset discussed in the previous sections. Based on the small number of clusters aged ~ 1 Gyr for which comparison data is available in the literature, we tentatively conclude that our broad-band SED analysis may have led to underestimates of the cluster ages for $\log(\text{Age}/\text{yr}) \simeq 9$,

in a similar sense as seen by H03. This tentative conclusion is supported by Fig. 5a, where our new age determinations appear somewhat lower than those determined from CMD analysis or spectral features for these ages.

Based on this comparison with independently determined ages for subsamples of LMC clusters, we conclude that our broad-band SED fits yield reliable ages, with statistical absolute uncertainties within $\Delta \log(\text{Age}/\text{yr}) \simeq 0.4$ overall, based on the scatter about the lines of equality. Thus, in addition to our conclusion in de Grijs et al. (2005) that we can retrieve prominent features in the cluster age distribution to within $\Delta \langle \log(\text{Age}/\text{yr}) \rangle \leq 0.35$, we have now also shown that the *intrinsic* statistical uncertainties involved in cluster age determinations based on broad-band SEDs are of a very similar magnitude.

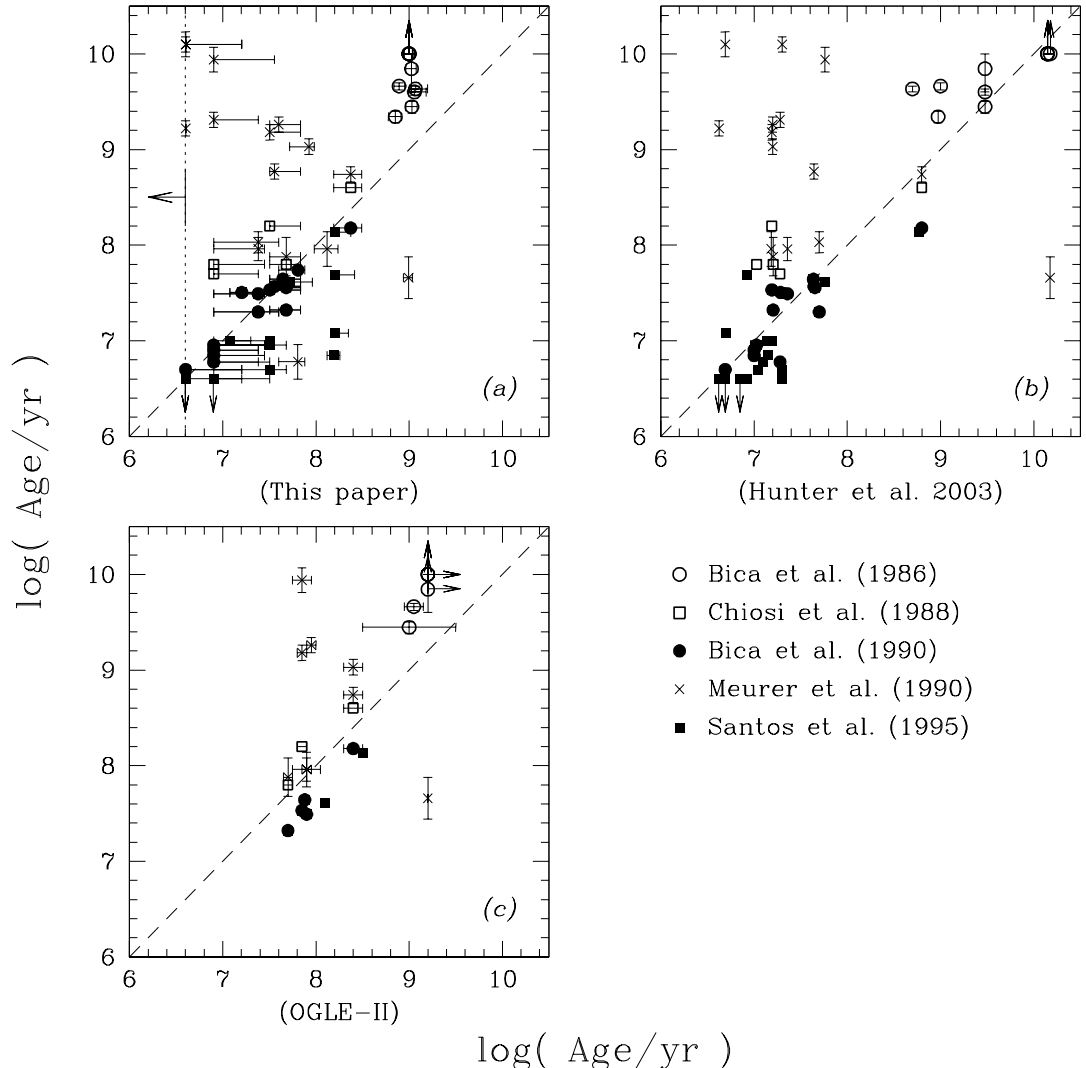


Figure 4. Comparison with other age determinations, based on broad-band photometry.

3 CLUSTER FORMATION AND DISRUPTION RATES

Using the newly determined and improved age estimates for the largest LMC cluster sample spanning the most extensive age and mass ranges to date, we now have the means to constrain the past cluster formation rate (CFR), as well as the effects of cluster disruption, to unprecedented detail.

3.1 Derivation of the characteristic cluster disruption time-scale

In Fig. 6a we display the number of clusters formed per unit age range. Evolutionary fading, as predicted by stellar population synthesis models, will cause this number to slowly decline from the youngest ages upward. This effect is shown by the dashed line in Fig. 6a, of which the slope is entirely determined by the details of stellar population synthesis; we have only shifted this line to best match the data points for $\log(\text{Age/yr}) \leq 8$. Both internal and external ef-

fects, such as two-body relaxation, disk and bulge shocking, and the tidal effects caused by the underlying galactic gravitational potential (even in the low-density environment of the LMC; cf. Lamers, Gieles & Portegies Zwart 2005), leading to tidal stripping and to evaporation of a fraction of the low-mass cluster stars, will result in the (gradual) dissolution of star clusters. Simple (instantaneous) disruption theory (Boutloukos & Lamers 2003) predicts that, assuming a constant CFR and that the characteristic cluster disruption time-scale is a function of cluster mass, the effects of cluster disruption will dominate from a certain age onwards, giving rise to the characteristic double power-law seen in Fig. 6a.

The location of the crossing point of the fading and disruption lines in Fig. 6a, denoted by “ t_{cross} ”, is a key ingredient to derive the characteristic cluster disruption time-scale for a given cluster population (Boutloukos & Lamers 2003). The other parameters required to derive this time-scale are the limiting magnitude, $M_V = -3.5$ mag (H03), $E(B - V) = 0.10$ mag or $A_V = 0.41$ mag (Section 2),

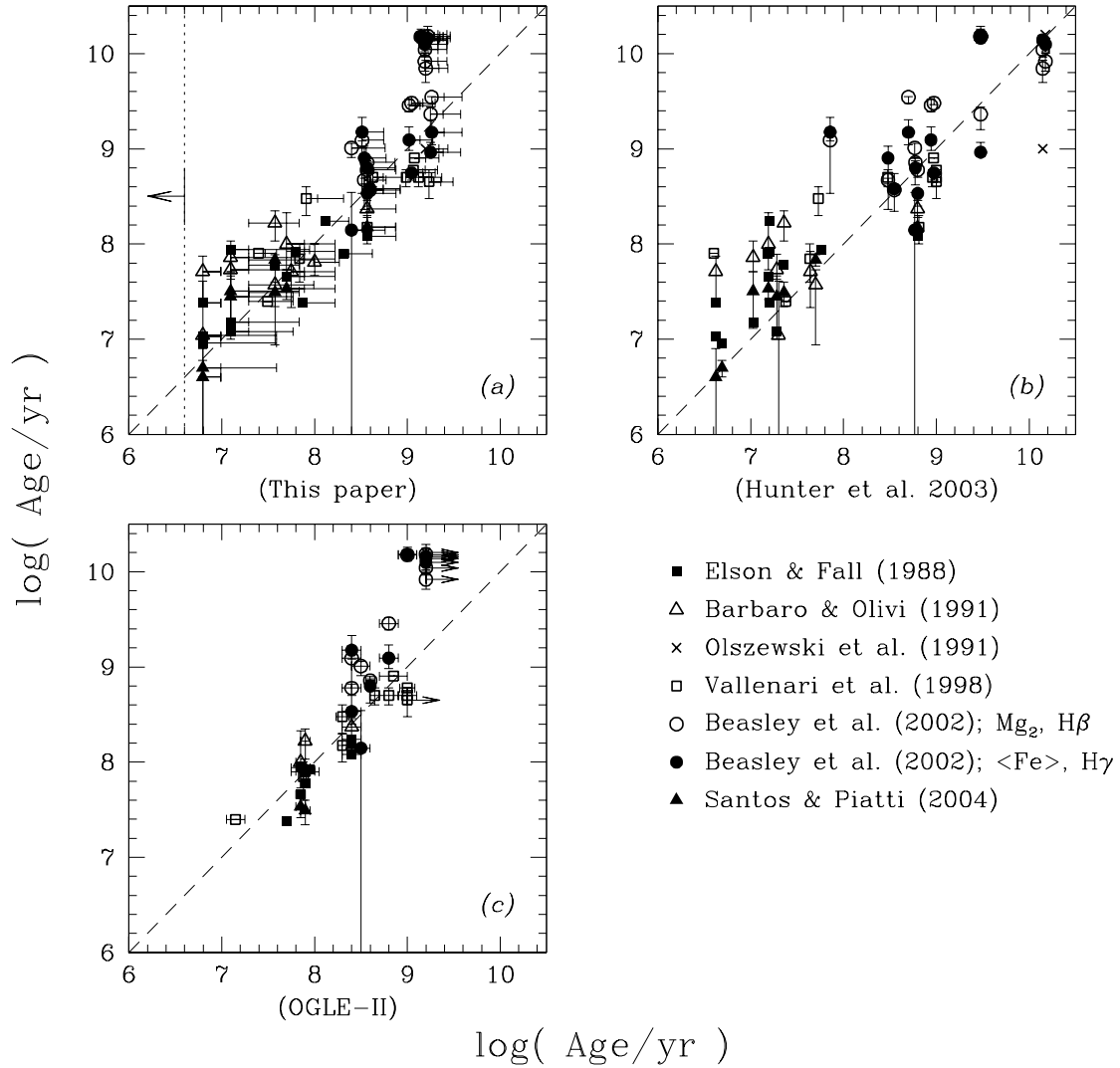


Figure 5. Comparison with other age determinations, based on either spectral features or CMD fitting.

$(m - M)_{\text{LMC}} = 18.48$ mag, and the reference magnitude, $M_V^{\text{ref}} = -11.3668$ mag, for a $10^4 M_{\odot}$ cluster at an age of 10^8 yr, which we obtained from the GALEV models for $Z = 0.4 Z_{\odot}$, assuming a “standard” Salpeter-like stellar IMF from 0.15 to $\sim 70 M_{\odot}$. For the crossing time we find $\log(t_{\text{cross}}/\text{yr}) = 8.10 \pm 0.05$, where the uncertainty is a combination of the uncertainty in the exact vertical level of the fading line, and the uncertainty regarding exactly when cluster disruption is significantly more important than fading. In order to assess the latter uncertainty, we applied a linear regression to the data points for $\log(\text{Age}/\text{yr}) \geq 8.2$ and 8.4, respectively, resulting in the dotted and dash-dotted fits in Fig. 6a. We note that for these fits we have omitted the data points in the LMC’s age gap, between 3 and 13 Gyr (see Section 3.2), since these would obviously violate the underlying assumption of a constant CFR.

In addition, we need the slope of the fading line (-0.648 ; from stellar population synthesis modelling) and the exact mass dependence of the disruption time-scale, γ , defined

as $t_{\text{dis}} \propto M_{\text{cl}}^{\gamma}$ (Boutloukos & Lamers 2003), in order to derive the characteristic disruption time-scale. Boutloukos & Lamers (2003) derived $\gamma = 0.62$ from observations of a small but diverse sample of galaxies containing rich cluster systems. Using these parameters as our input, we derive a characteristic cluster disruption time-scale for a $10^4 M_{\odot}$ cluster of $\log(t_4^{\text{dis}}/\text{yr}) = 9.9 \pm 0.1$. This is in good agreement with Boutloukos & Lamers (2002), who found $\log(t_4^{\text{dis}}/\text{yr}) = 9.7 \pm 0.3$ for a smaller sample of 478 clusters within 5 kpc from the centre of the LMC, in the age range $7.8 \leq \log(\text{Age}/\text{yr}) \leq 10.0$ (data from Hodge 1988), while our result is also qualitatively consistent with H03 who noticed very little destruction of clusters on the high-mass end. This is not unexpected, considering the low-density environment in which these clusters are found (cf. Lamers et al. 2005).

Even with recent improvements (e.g., Gieles et al. 2005) to the simple model of Boutloukos & Lamers (2003), the characteristic cluster destruction time-scales resulting from a more sophisticated, non-instantaneous destruction process

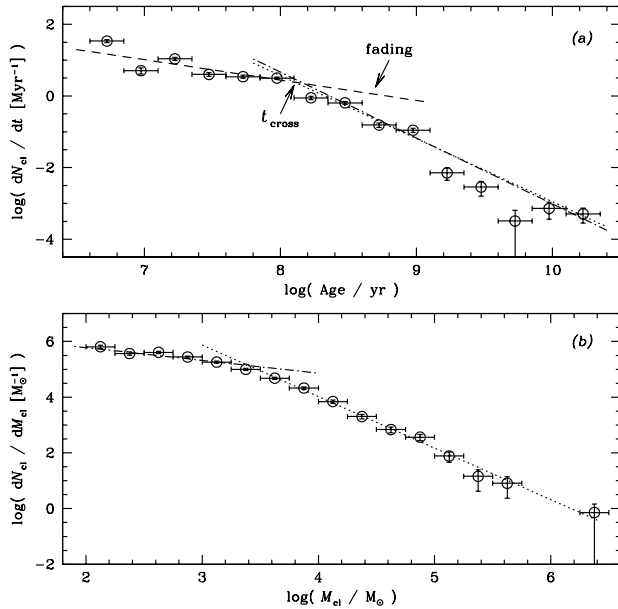


Figure 6. (a) – The LMC cluster formation rate (in number of clusters per Myr) as a function of age. The dashed line is the least-squares power-law fit to the fading, non-disrupted clusters, for a constant ongoing cluster formation rate. The dotted and dash-dotted lines are the disruption lines for the most likely age ranges where disruption may dominate evolutionary fading, as discussed in the text; (b) – Mass spectrum of the LMC clusters (number of clusters per unit mass range); the dotted line represents a power-law fit to the CMF that is as yet unaffected by disruption (see text); the slope of the dash-dotted line (which was shifted vertically to match the observational data) is entirely determined by the initial CMF slope determined from the dotted line, and stellar population synthesis, as described in the text.

are very similar to those based on the simple method (see Lamers et al. 2005 for a detailed comparison, in particular their table 1).

Finally, for completeness and a full assessment of the uncertainties involved, we need to address the effects of possibly having underestimated the ages of the oldest sample clusters. The ages of the oldest LMC clusters are well-known from detailed *Hubble Space Telescope*-based studies (e.g., Olsen et al. 1998) to all have essentially the same age of $\log(\text{Age}/\text{yr}) \simeq 10.1$. Therefore we reanalyzed Fig. 6b, now assuming this uniformly old age for all clusters for which we determined $\log(\text{Age}/\text{yr}) \geq 9.5$. Under this assumption, the resulting crossing time requires adjustment by $\Delta \log(t_{\text{cross}}/\text{yr}) \simeq -0.05$, leading to a lower limit to the characteristic disruption time-scale of $\log(t_4^{\text{dis}}/\text{yr}) = 9.8 \pm 0.1$, which is still in very good agreement with the earlier determination by Boutloukos & Lamers (2002).

Our analysis in this section depends on the key assumption that the CFR has remained approximately constant for the entire lifetime of the LMC star cluster system, with the exception of the time span covered by the age gap. That this assumption is justified to first order is supported by two additional lines of evidence: (i) the disruption lines in Fig. 6a are representative of the full LMC cluster sample for ages of $\log(\text{Age}/\text{yr}) \gtrsim 8.1$, whether or not we include the

oldest clusters that may possibly have formed at a different CFR (if we leave out the oldest clusters, the main effect is that the slope of the disruption line becomes less well constrained); (ii) the slope of the disruption line in either case corresponds to a mass dependence of the LMC cluster disruption time-scale of $t_{\text{dis}} \propto M_{\text{cl}}^{\gamma=0.56 \pm 0.07}$, which is – within the uncertainties – well inside the approximately universal proportionality found by Boutloukos & Lamers (2003) for a range of galaxies in the local Universe, $\gamma = 0.62 \pm 0.06$.

3.2 The LMC cluster formation rate

In Fig. 7 we show the distribution of the full LMC cluster sample in the (age vs. mass) plane. For reasons of clarity, we have not included error bars in this figure. Overplotted is the 50 per cent completeness limit based on stellar population synthesis for single-burst (“simple”) stellar populations (appropriate in the context of star clusters), for an estimated ~ 50 per cent completeness limit of $M_V = -3.5$ mag (H03), assuming a distance modulus to the LMC of $(m - M)_0 = 18.48$ mag, and no extinction. For a nominal extinction of $A_V = 0.1$ mag (assuming the Calzetti extinction law), the equivalent detection limit will shift to higher masses by $\Delta \log(M_{\text{cl}}/\text{M}_\odot) = 0.04$, which is well within the uncertainties associated with our mass determinations.

For a constant CFR, we expect the number of data points to increase gradually and evenly from young to old ages in the logarithmic representation of Fig. 7. Any obviously clumped subsets of data points may indicate either artifacts caused by our computational routines, or real deviations from a constant CFR. The effects of using interpolation of discrete isochrones for the determinations of cluster ages, and the resulting artifacts in age–mass space have been discussed extensively by Bastian et al. (2005) and Gieles et al. (2005). Based on their discussions, two features in Fig. 7 in particular can be attributed to artifacts caused by the fitting procedures: (i) the large density of clusters at $\log(\text{Age}/\text{yr}) = 6.6$ is simply caused by the fact that our youngest isochrone is at an age of 4 Myr (we are limited by the age range spanned by the Padova isochrones on which the GALEV SSP models are based), and younger clusters would therefore be assigned the minimum model age; (ii) the apparent overdensity around $\log(\text{Age}/\text{yr}) = 7.2$ is caused by the discreteness of the isochrones in this age range, where rapid changes occur in realistic stellar populations; it was also noted by Gieles et al. (2005) and Fall et al. (2005). Fortunately, however, from their age and mass determinations of artificial cluster populations using very similar procedures as done here, Gieles et al. (2005) find that they can retrieve the ages and masses of, respectively, 87 and 97 per cent of their input clusters to within 0.4 dex in $\log(\text{Age}/\text{yr})$ and $\log(M_{\text{cl}}/\text{M}_\odot)$, respectively (see also Fall et al. 2005). These retrieval rates are based on the assumption of a constant CFR, and an initial power-law CMF with exponent $\alpha = -2$.

In addition to these artifacts, we inspected two other apparent overdensities in Fig. 7, at $(7.8 \leq \log(\text{Age}/\text{yr}) \leq 8.0, 2.8 \leq \log(M_{\text{cl}}/\text{M}_\odot) \leq 3.4)$ and $8.2 \leq \log(\text{Age}/\text{yr}) \leq 8.4$ (for the full mass range), by displaying the locations of these cluster subsamples across the LMC. Neither of these apparent overdensities are associated with localised enhanced CFRs. In fact, any sufficiently large age and mass range (i.e., covering at least twice the typical uncertainty in age

and mass, following the Nyquist sampling theorem) shows a fairly homogeneous and relatively continuous (in terms of the cluster ages) distribution of star clusters across the disk of the LMC. We note, as a caveat, that the H03 cluster sample does not cover the entire LMC (e.g., it does not cover the dense LMC bar region), although Massey (2002) and H03 argue that their fields are representative of the LMC stellar (and cluster) population as a whole.

The last tidal encounter between the LMC and the Small Magellanic Cloud (SMC) occurred most likely about 0.2 to 0.5 Gyr ago (e.g., Heller & Rohlfs 1994; Gardiner & Noguchi 1996). One rotation period of the LMC corresponds to ~ 250 Myr (Grebel & Brandner 1999), or $\log(t_{\text{LMC}}^{\text{orb}}/\text{yr}) \simeq 8.4$. This implies that if an apparent feature in age–mass space at an age of $\log(\text{Age}/\text{yr}) \simeq 7.9$ was triggered by the LMC-SMC encounter, but corresponds to a spatial distribution of its clusters that is smooth and homogeneous across the LMC disk (i.e., at all radii), rotational mixing will not have had enough time for this to have happened, or at best marginally so. While such a gravitational interaction could, in principle, have triggered a galaxy-wide burst of cluster formation in the LMC, we would still expect to see a clearly enhanced population of clusters in a relatively narrow age range in such a case (cf. de Grijs et al. 2003a,b for the equivalent diagnostics in M82). Lacking better age resolution for a larger distinct cluster subpopulation, we cannot conclude with sufficient certainty that the last encounter between the LMC and the SMC was significantly strong to have triggered the formation of a well-defined cluster population in the LMC as a result; alternative triggering mechanisms may have been responsible for the formation of the smoothly distributed clusters at young(er) ages.

The only real *underdensity* of data points is the well-known LMC cluster age gap, between ~ 3 and 13 Gyr (e.g., Da Costa 1991; Geisler et al. 1997; Rich et al. 2001; Piatti et al. 2002; Bekki et al. 2004), which is well reproduced in our broad-band age redeterminations. We note that possible other underdensities in Fig. 7 occur (i) close to the 50 per cent completeness limit and (ii) for low masses, where we have to take stochastic sampling effects of the stellar initial mass function (IMF) into account; these effects act in the sense that a cluster of low mass may be dominated by a small number of high(er)-mass, and therefore high(er)-luminosity stars, which in turn will cause the photometric age to be (somewhat) overestimated. The exact amount of this depends sensitively on the cluster mass (see Section 4 below) and age. In particular, stochastic effects will be most pronounced in the age ranges where rapid evolutionary stages show up in stellar models, such as the appearance of red supergiants at ages around 8–12 Myr (e.g., Girardi & Bica 1993; Santos & Frogel 1997). Clusters that have reached ages of several $\times 10^7$ yr will be populated by a significant fraction of post-main sequence stars, and suffer less from stochastic effects in optical passbands, even if they are of low mass (e.g., Girardi & Bica 1993; Santos & Frogel 1997). The appearance of thermally-pulsing asymptotic giant branch stars around ages of ~ 1 Gyr can potentially give rise to large stochastic IMF sampling effects. However, these are most important at near-infrared wavelengths, and of lower importance at the optical wavelengths used for the age and mass estimates in this paper. Additional, yet circumstantial supporting evidence for this statement is provided by

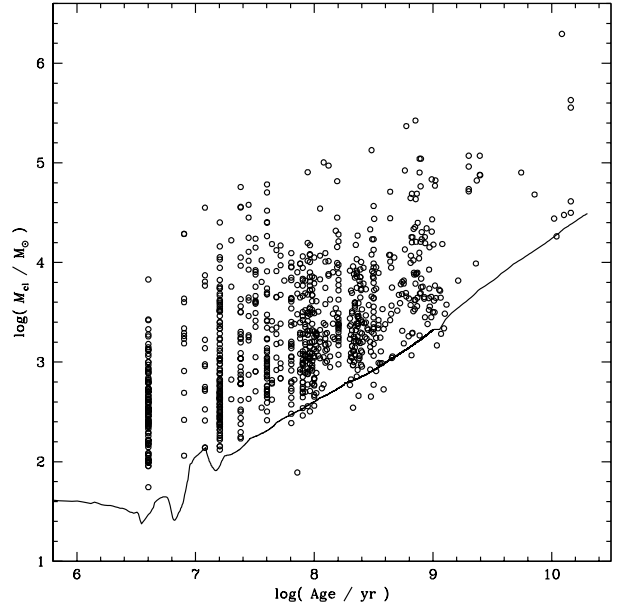


Figure 7. Distribution of the LMC clusters in the (age vs. mass) plane. Overplotted is the expected detection limit based on stellar population synthesis for a completeness limit of $M_V = -3.5$ mag (H03), assuming no extinction. For a nominal extinction of $A_V = 0.1$ mag (assuming the Calzetti attenuation law), the detection limit will shift to higher masses by $\Delta \log(M_{\text{cl}}/M_{\odot}) = 0.04$, which is well within the uncertainties associated with our mass determinations. The features around 10 Myr are caused by the appearance of red supergiants in the models.

the age and mass distribution shown in Fig. 7, where we do not detect any significant under or overdensity *in mass* of clusters at or close to ages of $\log(\text{Age}/\text{yr}) \sim 9.0$, although such effects could – to some extent – be masked by the relatively small number ($\lesssim 100$) of clusters in the logarithmic age interval [8.8,9.2].

An alternative method to portray the CFR is shown in Fig. 6a, where we display the number of clusters formed per unit age range. If we omit the three data points in the age gap, the remaining data points for $\log(\text{Age}/\text{yr}) \gtrsim 8$ are well approximated by a linear relationship. Since a linear relationship is predicted if the CFR has been constant, this approach shows the approximate validity of this assumption once again. If we assume that the CFR in the cluster age gap has also been constant, although at a (much) lower level (cf. H03), then we derive that the ratio of the CFR before and after the cluster age gap to that in the period between ~ 3 and 13 Gyr, is about $(5 \pm 1) : 1$. H03, considering the upper cluster masses, and assuming that the mass of the most massive cluster is determined by size-of-sample effects (which is approximately valid; H03), derived an equivalent ratio of ~ 10 , although with large uncertainties. In view of the independent methods used by H03 and us, based on entirely different diagnostics, these results are in reasonable agreement.

Finally, H03 suggested that the oldest sample clusters represent a separate population from the younger LMC clusters. They state that lower-mass old clusters could have been

observed but are not in practice. However, our new age and mass determinations do not concur with this result; Fig. 6 shows that our 50 per cent completeness limit describes the lower mass limit of the entire cluster sample up to the oldest ages very well. Similarly, the upper mass limit of the oldest clusters is commensurate with the upper mass limit expected from size-of-sample effects (cf. H03), and does not require that the oldest clusters represent a separate population. However, because of the small number of old clusters, we cannot draw any firmer conclusions on this issue based on the information at hand.

4 IMPLICATIONS FOR THE CLUSTER MASS FUNCTION AS A FUNCTION OF AGE

In Fig. 6b we show the LMC cluster mass distribution in a way that allows us to assess the importance of disruption processes for the sample, in the presence of an age-dependent detection (completeness) limit (see Boutloukos & Lamers 2003). As we showed in de Grijs et al. (2003d), the slope of the distribution for the highest masses is in essence a projection of the *initial* CMF, provided that we can prove that (semi-instantaneous) disruption will not yet have had the time to act on these masses.

In Table 2 we list the derived slopes for mass ranges from the minimum masses indicated to the highest masses present in our sample. We note that, for $\log(M_{\text{cl}}/\text{M}_{\odot}) \gtrsim 3.0$ the CMF slopes derived are very stable (except for the highest mass ranges, where the small number of clusters affects the results), resulting in an initial CMF slope of $\alpha = -1.85 \pm 0.05$ as our best determination. This is significantly (at the 3σ level) smaller than the “universal” initial CMF slopes of $\alpha = -2$ often found in interacting and starburst galaxies, and used as the basis for theoretical models of the evolution of young cluster populations (see, e.g., de Grijs et al. 2003d for a review). We will discuss the implications of this result in the context of our discussion of Fig. 8 below. We note that for $\log(M_{\text{cl}}/\text{M}_{\odot}) \geq 3.0$, $\log(t_{\text{dis}}/\text{yr}) \geq 9.3$; in this age range, the clusters that would have been affected by ongoing (semi-instantaneous) disruption have already faded to below the adopted completeness limit, so that we conclude that here we are indeed observing the *initial* CMF slope. We note that the low density of the LMC field, while to some small extent effective in tidal stripping and evaporation, does not lead to a significant breakdown of our assumption of (almost) instantaneous disruption: most of the evaporated and stripped stars will be of low mass, which hence contribute negligibly to the integrated luminosities we use for our analysis.

Using the value of $\alpha = -1.85$, and the fading parameter $\zeta = 0.648$ (where fading of a cluster’s flux, F_{λ} , is defined as $F_{\lambda} \sim t^{-\zeta}$) from stellar population synthesis (Boutloukos & Lamers 2003), the predicted power-law slope for the low-mass range is $(1/\zeta) - |\alpha|$. This slope is shown as the dash-dotted line in Fig. 6b, and matches the observed mass distribution remarkably well (we have only applied a vertical shift to the slope in order to match the cluster numbers in the distributions).

Alternatively, we can assess the CMF and its possible evolution by examining the CMFs of well-defined and well-understood subsamples covering restricted mass ranges.

Table 2. Mass range-dependent LMC cluster mass function slopes, based on magnitude-limited sampling (Fig. 6b).

$\log(M_{\text{cl}}/\text{M}_{\odot})_{\text{min}}$	CMF slope	
	$dN_{\text{cl}}/d(M_{\text{cl}}/\text{M}_{\odot})$	$d\log(N_{\text{cl}})/d\log(M_{\text{cl}}/\text{M}_{\odot})$
2.25	-1.59 ± 0.08	-0.59 ± 0.08
2.50	-1.67 ± 0.06	-0.67 ± 0.06
2.75	-1.73 ± 0.06	-0.73 ± 0.06
3.00	-1.85 ± 0.05	-0.85 ± 0.05
3.25	-1.83 ± 0.05	-0.83 ± 0.05
3.50	-1.85 ± 0.06	-0.85 ± 0.06
3.75	-1.86 ± 0.08	-0.86 ± 0.08
4.00	-1.84 ± 0.09	-0.84 ± 0.09
4.25	-1.81 ± 0.12	-0.81 ± 0.12
4.50	-1.80 ± 0.15	-0.80 ± 0.15
4.75	-1.78 ± 0.21	-0.78 ± 0.21
5.00	-1.55 ± 0.19	-0.55 ± 0.19

Following Fall et al. (2005), in Fig. 8 we present mass-limited LMC cluster subsamples, which are potentially physically more informative than magnitude-limited subsamples. Mass-limited sample are less biased toward young clusters than magnitude-limited samples. This is a novel approach for the LMC star cluster system. In essence, a mass-limited statistically complete sample of clusters implies an imposed age limitation as well, so that for increasing masses, the upper age limit increases, and so does the median age of the subsample. The mass and age ranges used for the construction of the CMFs in Fig. 8 are listed in Table 3, as well as in the individual panels in the figure.

The error bars indicate the simple Poissonian uncertainties, and the vertical dotted lines indicate the minimum mass limits adopted for a particular cluster subsample; in all cases the corresponding age limits are well below the expected disruption time-scales for even the least massive clusters in a given sample. In Table 3 we also include the CMF slopes we derive from each cluster subsample. For samples up to $\log(\text{Age/yr}) \leq 8.7$, we use a mass fitting range of $\log(M_{\text{cl}}/\text{M}_{\odot}) \geq 3.0$; for the remaining subsamples we use the full mass range available for the fits. We note explicitly that using a lower age limit of $\log(\text{Age/yr}) = 6.8$ or 7.2, in order to avoid the artifact caused by the limited age resolution of the isochrones used for the analysis does *not* alter these results significantly (or may even strengthen these results, albeit marginally).

The key result is that, for clusters with $\log(M_{\text{cl}}/\text{M}_{\odot}) \geq 3.0$ and $\log(\text{Age/yr}) > 7.80$ (i.e., for all but the two youngest subsamples), the CMF slopes are very close to unity (see also H03 for similar results for the high-mass wings of their age-limited CMFs¹), which in this parameter space corresponds to an initial CMF slope of $\alpha \simeq -2$ (see also the final column in Table 2 for a direct comparison). However, the youngest

¹ We note that H03 did not take the age and mass-dependent completeness limits into account for the construction of their CMFs (their fig. 6). However, a close comparison between the mass fitting ranges they used on the one hand with Fig. 7 on the other reveals that they determined the CMF slopes well inside the statistically complete mass range for each age-limited cluster subsample. It is therefore not surprising, indeed rather encouraging, that the results we obtain for a larger number of subsamples for different age and mass ranges agree very well with those of H03.

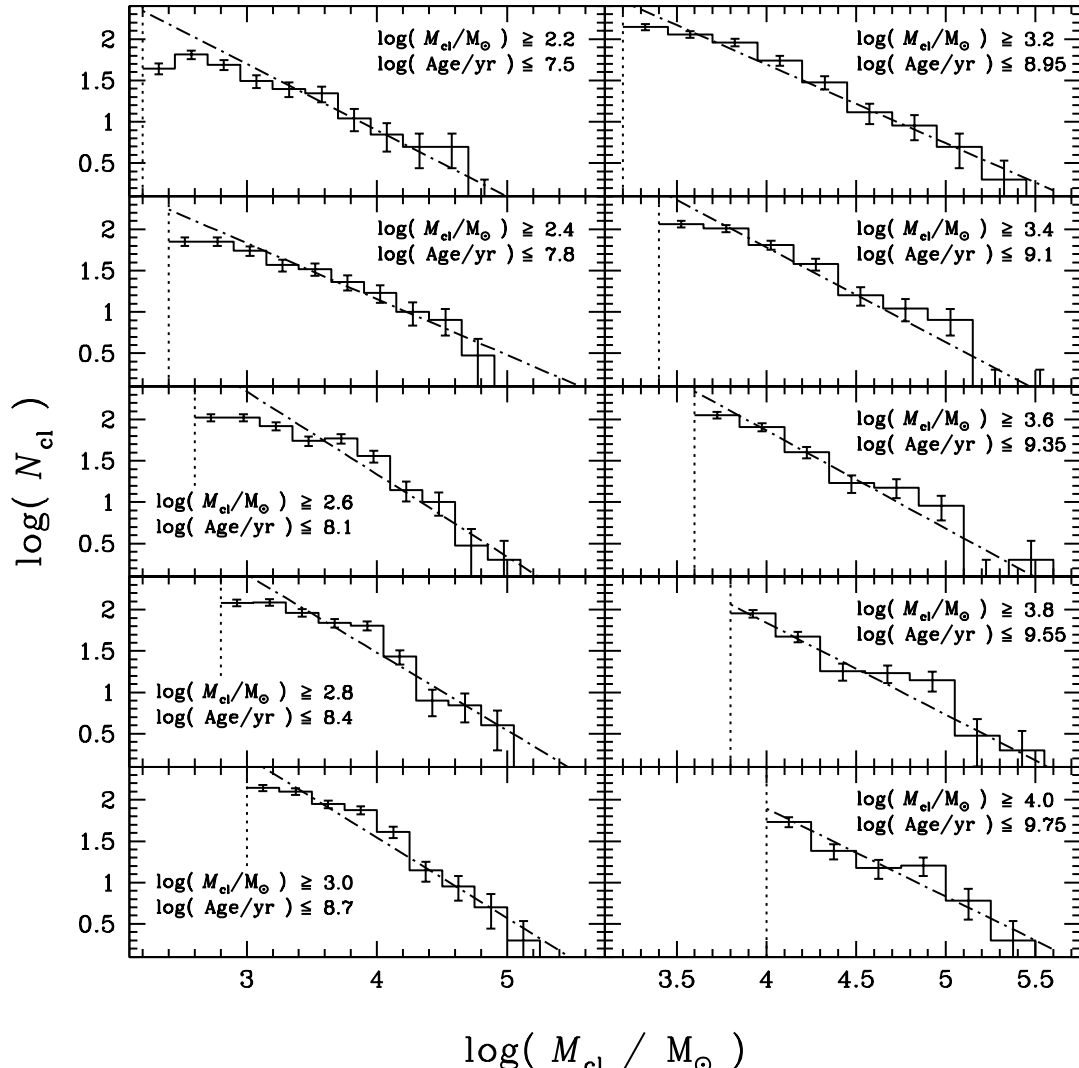


Figure 8. CMFs for statistically complete LMC cluster subsamples. Age and mass ranges are indicated in the panel legends; the vertical dotted lines indicate the lower mass limits adopted. Error bars represent simple Poissonian errors, while the best-fit lines were obtained for $\log(M_{\text{cl}}/M_{\odot}) \geq 3.0$ for $\log(\text{Age}/\text{yr}) \leq 8.7$, and for the full available mass range for older maximum ages. Table 3 summarises the best-fit parameters.

two subsamples exhibit significantly shallower slopes for the same mass range (see also Elmegreen & Efremov 1997), while for $\log(M_{\text{cl}}/M_{\odot}) < 3.0$ the observed CMFs turn down even more significantly below the linear slopes indicated. We note that the observed effect goes well beyond that expected from uncertainties in the data's completeness limit: an uncertainty in the completeness limit of 0.5 mag translates to an uncertainty in mass of only $\Delta \log(M_{\text{cl}}/M_{\odot}) = 0.2$. As the Poissonian error bars indicate, this flattening of the CMF slope is unlikely to be caused by small-number statistics either, while cluster disruption or variable external tidal effects are expected to have had a more important effect on the low-mass extreme of *older* clusters than on the younger clusters for which we notice this discrepancy. Thus, this observation is contrary to theoretical predictions if the initial CMF of the LMC cluster system were a power-law distribution modified by cluster disruption processes. We recall that

based on our magnitude-limited sample analysis (Fig. 6b), we also concluded that the initial CMF slope appeared to be significantly shallower, at the 3σ level, than the power-law slope, $\alpha = -2$, expected for young star cluster systems.

Since we observe this behaviour towards the low-mass end for all mass and age subsets of the full mass-limited cluster sample that include masses $\log(M_{\text{cl}}/M_{\odot}) \lesssim 3$, as well as in our magnitude-limited sample, random stochastic effects are unlikely to be the primary cause (see also Girardi & Bica 1993; Santos & Frogel 1997). It is likely that this is a real effect (see also Elmegreen & Efremov 1997), and that the CMF slopes flatten significantly for younger ages and lower-mass clusters in the LMC. Elmegreen & Efremov (1997) argue that the younger clusters are mostly unbound OB associations (supporting Bica et al. 1996), of which some 90 per cent will disperse by the time their constituent stars will reach an age of $\sim 10^8$ yr. This is consistent with modern

Table 3. LMC cluster mass function slope as a function of minimum mass and maximum age, based on mass-limited samples (Fig. 8).

$\log(M_{\text{cl}}/\text{M}_{\odot})_{\text{min}}$	$\log(\text{Age}/\text{yr})_{\text{max}}$	CMF slope [$d \log(N_{\text{cl}})/d \log(M_{\text{cl}}/\text{M}_{\odot})$]
2.2	7.50	-0.80 ± 0.10
2.4	7.80	-0.68 ± 0.06
2.6	8.10	-1.00 ± 0.10
2.8	8.40	-0.94 ± 0.10
3.0	8.70	-0.98 ± 0.08
3.2	8.95	-0.95 ± 0.06
3.4	9.10	-1.15 ± 0.11
3.6	9.35	-1.18 ± 0.14
3.8	9.55	-1.10 ± 0.12
4.0	9.75	-1.06 ± 0.15

ideas on the formation and dissolution of star clusters within the first $\sim 10^7$ yr of their existence; most ($\sim 70 - 90$ per cent) of these newly formed clusters will disperse on these time-scales, a process coined “infant mortality” (e.g., Boily & Kroupa 2003; Vesperini & Zepf 2003; Whitmore 2004; Bastian et al. 2005; Mengel et al. 2005; see also Tremonti et al. 2001). If the process of infant mortality is mass dependent (but see Whitmore 2004 for counterarguments), in the sense that the lowest-mass clusters will dissolve preferentially, the result will be a *flattening* of the CMF slopes with increasing mean age, which is contrary to the apparent change of slope in Fig. 8. Whether or not the youngest ($\lesssim 10$ Myr old) clusters will dissolve because of this infant mortality scenario, the significant differences among the LMC’s CMF slopes as a function of age are predominantly driven by the youngest subset of our cluster sample.

Thus, these results may imply that the initial CMF slope of the *combined* (i.e., both bound and unbound) LMC cluster system is *not* well represented by a power-law, although we cannot disentangle the unbound from the bound clusters at the youngest ages. In addition, we recently presented observational evidence and theoretical arguments against an initial power-law CMF in M82’s intermediate-age starburst region, M82 B (de Grijs, Parmentier & Lamers 2005), and in favour of an initial log-normal CMF in the Antennae interacting system, NGC 4038/39 (Anders et al. 2005). Our detailed analysis of the LMC cluster mass distributions as a function of age and mass may therefore have uncovered supporting new evidence that star clusters – at least in the low-density environment of the LMC – may not form following a power-law distribution that holds strength down to masses much below a few $\times 10^3$ M_{\odot} , where the power-law fits to the subsamples in Fig. 8 break down.

5 SUMMARY AND CONCLUSIONS

By combining integrated properties with resolved stellar population studies, the LMC cluster system offers the unique chance to independently check the accuracy of age (and corresponding mass) determinations based on broad-band SEDs. In this paper, we have reanalyzed the broad-band LMC cluster SEDs based on the data of Massey (2002) and H03, using a newly developed SED analysis approach. We compare our new age determinations with (i) those of H03 using the same data set but a different approach, and (ii) those of Pietrzyński & Udalski (2000) using CMD fitting, in

order to set the tightest limits yet on the accuracy of (absolute) age determinations based on broad-band SEDs, and therefore on the usefulness of such an approach.

We note a significant systematic effect between the age differences of H03 on the one hand, and those of both the OGLE-II team and our own redeterminations on the other. It appears that these systematic differences are caused by H03’s conversions of the photometry to a different filter system. We emphasize and warn that the *actual* filter systems used for the observations should be used for the most accurate parameter analysis, instead of using filter conversion equations, in order to achieve more accurate derivations of the cluster ages and the corresponding masses.

Based on this comparison, and additionally on a detailed assessment of the age-metallicity and age-extinction degeneracies, we conclude that our broad-band SED fits yield reliable ages, with statistical *absolute* uncertainties within $\Delta \log(\text{Age}/\text{yr}) \simeq 0.4$ overall. Thus, in addition to our conclusion in de Grijs et al. (2005) that we can retrieve prominent features in the cluster age distribution to within $\Delta \langle \log(\text{Age}/\text{yr}) \rangle \leq 0.35$ using a variety of approaches based on broad-band SEDs modelling, we have now also shown that the associated *intrinsic* statistical uncertainties involved in cluster age determinations are of a very similar magnitude.

The LMC’s CFR has been roughly constant outside of the well-known age gap between ~ 3 and 13 Gyr, when the CFR was a factor of ~ 5 lower (assuming a roughly constant rate during the entire period). There are no clear observational signatures of an enhanced CFR associated with the last tidal encounter between the LMC and the SMC, while we argue that the combination of the relevant time-scales, i.e., the LMC’s rotation period and the time since the last LMC-SMC encounter, has been insufficient to wash out any such signatures, if they had been present. An alternative triggering mechanism for the young(er) clusters may be needed.

Using a simple approach to derive the characteristic cluster disruption time-scale, we find that $\log(t_4^{\text{dis}}/\text{yr}) = 9.9 \pm 0.1$, where $t_4^{\text{dis}} = t_4^{\text{dis}}(M_{\text{cl}}/10^4 \text{M}_{\odot})^{0.62}$, for the LMC cluster system. This is consistent with earlier, preliminary work for a smaller cluster sample. This long characteristic disruption time-scale implies that hardly any of our LMC sample clusters are affected by significant disruptive processes, so that we are in fact observing the *initial* CMF. Using a variety of complementary techniques, we conclude that the older cluster (sub)samples show CMF slopes that are fully consistent with the $\alpha \simeq -2$ slopes generally observed in young star cluster systems. The youngest clusters in our sample show shallower slopes, at least below masses of a few $\times 10^3$ M_{\odot} , and possibly evidence for a turn-over. This is contrary to dynamical expectations and may imply that the initial CMF slope of the LMC cluster system as a whole is *not* well represented by a power-law down to the lowest masses, although we cannot disentangle the unbound from the bound clusters at the youngest ages.

ACKNOWLEDGMENTS

We thank Deirdre Hunter and Bruce Elmegreen for kindly providing us with their LMC cluster photometry, Phil

Massey for helpful discussions regarding the filter sets used, Jon Holtzman for sending us the unpublished Landolt KPNO filter transmission curves, and Uta Fritze-v. Alvensleben and Henny Lamers for useful comments. We acknowledge helpful comments on the OGLE-II cluster data from Andrzej Udalski and Grzegorz Pietrzyński. We also acknowledge research support from and hospitality at the International Space Science Institute in Berne (Switzerland), as part of an International Team programme. RdG is grateful for hospitality at the National Astronomical Observatories of the Chinese Academy of Sciences in Beijing – and in particular to Deng Li-Cai – where most of this work was completed; travel support was provided by the Royal Society under the UK’s Office of Science and Technology’s UK-China science network scheme, for one-to-one visits. This research has made use of NASA’s Astrophysics Data System Abstract Service.

REFERENCES

Anders P., Bissantz N., Fritze-v. Alvensleben U., de Grijs R., 2004, MNRAS, 347, 196

Anders P., Fritze-v. Alvensleben U., 2003, A&A, 401, 1063

Anders P., Bissantz N., Boysen L., de Grijs R., Fritze-v. Alvensleben U., 2005, Nature Physics, submitted

Barbaro G., Olivi F.M., 1991, AJ, 101, 922

Bastian N., Gieles M., Lamers H.J.G.L.M., Scheepmaker R.A., de Grijs R., 2005, A&A, 431, 905

Beasley M.A., Hoyle F., Sharples R.M., 2002, MNRAS, 336, 168

Bekki K., Couch W.J., Beasley M.A., Forbes D.A., Chiba M., Da Costa G.S., 2004, ApJ, 610, L93

Bica E., Alloin D., Santos J.F.C. Jr., 1990, A&A, 235, 103

Bica E., Dottori H., Pastoriza M., 1986, A&A, 156, 261

Boily C.M., Kroupa P., 2003, MNRAS, 338, 665

Boutloukos S.G., Lamers H.J.G.L.M., 2003, MNRAS, 338, 717

Boutloukos S.G., Lamers H.J.G.L.M., 2002, in: Extragalactic Star Clusters, IAU Symp. 207, Geisler D., Grebel E.K., Minniti D., (San Francisco: ASP), p.703

Calzetti D., 1997, AJ, 113, 162

Calzetti D., Armus L., Bohlin R.C., Kinney A.L., Koornneef J., Storchi-Bergmann T., 2000, ApJ, 533, 682

Calzetti D., 2001, PASP, 113, 1449

Cardelli J.A., Clayton G.C., Mathis J.S., 1989, ApJ, 345, 245

Charlot S., Bruzual A.G., 1991, ApJ, 367, 126

Chiosi C., Bertelli G., Bressan A., 1988, A&A, 196, 84

Da Costa G.S., 1991, in IAU Symp. 148, The Magellanic Clouds, Haynes R., Milne D., eds., (Dordrecht: Kluwer), p. 183

de Grijs R., O’Connell R.W., Gallagher J.S., 2001, AJ, 121, 768

de Grijs R., Bastian N., Lamers H.J.G.L.M., 2003a, MNRAS, 340, 197

de Grijs R., Bastian N., Lamers H.J.G.L.M., 2003b, ApJ, 583, L17

de Grijs R., Fritze-v. Alvensleben U., Anders P., Gallagher J.S. III, Bastian N., Taylor V.A., Windhorst R.A., 2003c, MNRAS, 342, 259

de Grijs R., Anders P., Lynds R., Bastian N., Lamers H.J.G.L.M., O’Neill E.J., Jr., 2003d, MNRAS, 343, 1285

de Grijs R., Anders P., Lamers H.J.G.L.M., Bastian N., Parmenier G., Sharina M.E., Yi S., 2005, MNRAS, 359, 874

de Grijs R., Parmentier G., Lamers H.J.G.L.M., 2005, MNRAS, in press (astro-ph/0509721; doi: 10.1111/j.1365-2966.2005.09640.x)

Elson R.A.W., Fall S.M., 1988, AJ, 96, 1383

Elmegreen B.G., Efremov Y.N., 1997, ApJ, 480, 235

Fall S.M., Chandar R., Whitmore B.C., 2005, ApJ, 631, L133

Fritze-v. Alvensleben U., 1998, A&A, 336, 83

Fritze-v. Alvensleben U., 1999, A&A, 342, L25

Gardiner L.T., Noguchi M., 1996, MNRAS, 278, 191

Geisler D., Bica E., Dottori H., Clariá J.J., Piatti A.E., Santos J.F.C., Jr., 1997, AJ, 114, 1920

Gieles M., Bastian N., Lamers H.J.G.L.M., Mout J.N., 2005, A&A, 441, 949

Girardi L., Bica E., 1993, A&A, 274, 279

Grebel E.K., Brandner W., 1999, in: New Views of the Magellanic Clouds, IAU Symp. 190, Chu Y.-H., Suntzeff N., Hesser J., Bohlender D., (San Francisco: ASP), p. 470

Heller P., Rohlfs K., 1994, A&A, 291, 743

Hodge P., 1988, PASP, 100, 576

Holtzman J.A., Burrows C.J., Casertano S., Hester J.J., Trauger J.T., Watson A.M., Worthey G., 1995, PASP, 107, 1065

Hunter D.A., Elmegreen B.G., Dupuy T.J., Mortonson M., 2003, AJ, 126, 1836 (H03)

Kurth O.M., Fritze-v. Alvensleben U., Fricke K.J., 1999, A&AS, 138, 19

Lamers H.J.G.L.M., Gieles M., Portegies Zwart S., 2005, A&A, 429, 173

Landolt A.U., 1992, AJ, 104, 340

Leitherer C., et al., 1999, ApJS, 123, 3 (Starburst99)

Leitherer C., Li I.-H., Calzetti D., Heckman T.M., 2002, ApJS, 140, 303

Massey P., 2002, ApJS, 141, 81

Mengel S., Lehnert M.D., Thatte N., Genzel R., 2005, A&A, 443, 41

Meurer G.R., Cacciari C., Freeman K.C., 1990, AJ, 99, 1124

Meurer G.R., Heckman T.M., Leitherer C., Kinney A., Robert C., Garnett D.R., 1995, AJ, 110, 2665

Miller B.W., Whitmore B.C., Schweizer F., Fall S.M., 1997, AJ, 114, 2381

Olsen K.A.G., Hodge P.W., Mateo M., Olszewski E.W., Schommer R.A., Suntzeff N.B., Walker A.R., 1998, MNRAS, 300, 665

Olszewski E.W., Schommer R.A., Suntzeff N.B., Harris H.C., 1991, AJ, 101, 515

Piatti A., Sarajedini A., Geisler D., Bica E., Clariá J.J., 2002, MNRAS, 329, 556

Pietrzyński G., Udalski A., 2000, AcA, 50, 337 (OGLE-II)

Reed B.C., 1985, PASP, 97, 120

Rich R.M., Shara M.M., Zurek D., 2001, AJ, 122, 842

Santos J.F.C., Jr., Bica E., Clariá J.J., Piatti A.E., Girardi L.A., Dottori H., 1995, MNRAS, 276, 1155

Santos J.F.C., Jr., Frogel J.A., 1997, ApJ, 479, 764

Santos J.F.C., Jr., Piatti A.E., 2004, A&A, 428, 79

Schlegel D.J., Finkbeiner D.P., Davis M., 1998, ApJ, 500, 525

Schulz J., Fritze-v. Alvensleben U., Möller C.S., Fricke K.J., 2002, A&A, 392, 1

Searle L., Sargent W.L.W., Bagnuolo W.G., 1973, ApJ, 179, 427

Searle L., Wilkinson A., Bagnuolo W.G., 1980, ApJ, 239, 803 (SWB)

Tremonti C.A., Calzetti D., Leitherer C., Heckman T.M., 2001, ApJ, 555, 322

Udalski A., Kubiak M., Szymański M., 1997, AcA, 47, 319

Udalski A., Soszyński I., Szymański M., Kubiak M., Pietrzyński G., Woźniak P., Źebrowski K., 1999, AcA, 49, 223

Vallenari A., Bettoni D., Chiosi C., 1998, A&A, 331, 506

Vesperini E., Zepf S.E., 2003, ApJ, 587, L97

Whitmore B.C., 2004, in: The Formation and Evolution of Massive Young Star Clusters, ASP Conf. Ser., vol. 322, Lamers H.J.G.L.M., Smith L.J., Nota A., eds., (ASP: San Francisco), p. 419